Bull. Chem. Soc. Ethiop. **2018**, 32(1), 89-100.
DOI: https://dx.doi.org/10.4314/bcse.v32i1.8

ISSN 1011-3924
Printed in Ethiopia

SYNTHESIS OF NEW NANO SCHIFF BASE COMPLEXES: X-RAY CRYSTALLOGRAPHY, THERMAL, ELECTROCHEMICAL AND ANTICANCER STUDIES OF NANO URANYL SCHIFF BASE COMPLEXES

Fahimeh Dehghani Firuzabadi[1], Zahra Asadi[1*] and Reza Yousefi[2]

[1]Department of Chemistry, College of Science, Shiraz University, Shiraz 71454, Iran
[2]Protein Chemistry Laboratory, Department of Biology, Shiraz University, 71454 Shiraz, Iran

(Received November 19, 2016; Revised January 15, 2018; Accepted January 23, 2018)

ABSTRACT. This study presents synthesis and characterization of new nano uranyl Schiff base complexes. Electrochemistry of these complexes showed a quasireversible redox reaction without any successive reactions. Furthermore, X-ray crystallography exhibited that beside the coordination of tetradentate Schiff base, one solvent molecule (dimethylformamide) was also coordinated. According to Coats-Redfern plots the kinetics of thermal decomposition of the studied complexes was first-order in all stages. Anticancer activities of the uranyl Schiff base complexes against cancer cell lines (Jurkat) was studied and determined by MTT (3-[4,5-dimethylthiazol-2-yl]-2,5-diphenyltetrazoliumbromide) assay. The results demonstrated that the complexes with aliphatic bridging units showed less anticancer activities than those having the aromatic units.

KEY WORDS: Uranyl Schiff base complex, Anticancer activities, Thermal studies, Electrochemistry; X-ray crystallography

INTRODUCTION

Studies show that Schiff bases and their complexes have many applications in the fields of catalysis [1, 2], synthesis [3], polymerization [4], epoxidation of olefins [5], degradation of dyes through decomposition of hydrogen peroxide and other reagents, textile industries [6], biological [7], and photochromic applications [8]. Coordination chemistry of uranyl salts is an area of chemistry that has been widely studied recently, especially when compared to the interest involving coordination compounds of the lanthanides, transition metals [9] and actinides of oxidation states +5 and +6 [10].

Unlike d-block oxo-cations, $[UO_2]^{2+}$ is stable over a wide pH range and can be identified in almost all uranium(VI) oxide solids. This species has a linear O=U=O structure, and the additional ligands coordinate to the central atom in the equatorial plane of UO_2^{2+}. The number of equatorial coordination sites varies between 3 and 6. The Schiff base ligands in uranyl Schiff base complexes bound in a tetradentate plane. A solvent molecule occupies the fifth coordinate site in the equatorial position [11]. The presence of the solvent can play an important role in the activation of the substrate in catalysis for acyl transfer, Michael-type addition of thiols, molecular recognition of urea derivatives, pyridine derivatives, amines, quinolines, nitriles, and other anions [12]. In our previous work [13], we investigated the effect of aromatic amines on the anticancer activity of the uranyl Schiff base complexes. Here we utilized the aliphatic amines in the synthesis of some new uranyl Schiff base complexes to find their anticancer activity. All the complexes were characterized by different techniques.

EXPERIMENTAL

Chemicals and apparatus

1,2-Ethylenediamine, 1,2-propylenediamine, 1,3-propylenediamine, 1,4-butylenediamine, uranylacetatedihydrate $UO_2(OAc)_2.2H_2O$, tetrabutylammunium perchlorate (Bu_4NClO_4), 2-

*Corresponding author. E-mail: zasadi@shirazu.ac.ir

hydroxy-1-naphthaldehyde, methanol, chloroform ($CHCl_3$), dimethylformamide (DMF), acetonitrile (CH_3CN), DMSO-d_6, potassium bromide (KBr) and $CDCl_3$ were purchased commercially and used without further purification.

The electronic absorption spectra were recorded using a Perkin-Elmer Lambda 2 spectrophotometer. FT-IR spectra were recorded by Shimadzu FTIR–8300 infrared spectrophotometer. The ^{1}H NMR spectra were recorded on a Bruker Avance DPX–250 spectrometer in DMSO−d_6 solvent using TMS as an internal standard at 250 MHz. Elemental microanalyses were obtained using a CHN Thermo-Finnigan Flash EA1112. BUCHI 535 instrument was used to obtain the melting point of the compounds. Thermal gravimetric analyses were recorded on Perkin-Elmer Pyris Diamond model. Electrochemical studies were obtained by using Auto lab 302N. A three-electrode system was utilized, i.e., a glassy carbon working electrode, a reference electrode (Ag/Ag^+ in TBAP/acetonitrile solution), and a Pt auxiliary electrode. The measurements of CV for CH_3CN solution containing uranyl complexes (1 mM) and TBAP (0.10 M) were carried out in the potential range from 0.2 V to -1.4 V. Tetrabutylammonium perchlorate (TBAP) was used as supporting electrolyte.

Incubator and ELISA reader (Bio-Tek's ELx808, USA) were used for anticancer studies. Transmission electron microscopy (TEM) images were obtained on a Zeiss EM10C transmission electron microscope using ACC voltage of 60 kV. The X-ray diffraction measurements were made on a STOE IPDS 2T diffractometer with graphite monochromated Mo-K_α radiation.

Synthesis of the ligands

All the tetradentate Schiff base ligands were prepared by condensation of diamines (1 mmol) and 2-hydroxy-1-naphthaldehyde (2 mmol) in methanol (25 mL). The mixture was refluxed for about 5 h. The products were washed with methanol and diethyl ether. All the Schiff base ligands were dried at 50 ºC under vacuum (Figure 1).

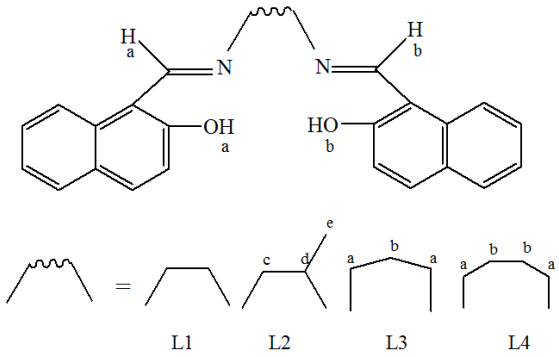

Figure 1. Structural representation of the Schiff base ligands.

H_2L1: N,N'-bis(naphthalidene)-1,2-ethylenediamine. Yield: 66%, color: yellow, m.p. >250 °C, anal. found (calc.): $C_{24}H_{20}N_2O_2$ (368.43): C, 78.64 (78.24); H, 5.47 (5.47); N, 8.02 (7.60). IR (KBr, cm^{-1}): 3469 (ν_{O-H}), 2953-3042 (ν_{C-H}), 1637 ($\nu_{C=N}$), 1540 ($\nu_{C=C}$), ^{1}H NMR: Schiff base was not soluble in DMSO or $CDCl_3$. UV-Vis (acetonitrile): λ_{max} (nm), ε ($M^{-1}cm^{-1}$) = 261 (15608), 269 (sh), 305 (11054), 400 (8629), 424 (9209).

H_2L2: N,N'-bis(naphthalidene)-1,2-propylenediamine. Yield: 78%, color: yellow, m.p. = 157-159 °C, anal. found (calc.): $C_{25}H_{22}N_2O_2$ (394.47): C, 79.49 (79.17); H, 5.71 (5.62); N, 7.51

(7.10). IR (KBr, cm^{-1}): 3433 (ν_{O-H}), 2931-3031 (ν_{C-H}), 1620 ($\nu_{C=N}$), 1542 ($\nu_{C=C}$), ^{1}H NMR (250 MHz, DMSO-d_6, room temperature): δ (ppm) = 1.34-1.42 (d, 3H, CH_3^e), 3.94 (m, 1H, CH^d), 4.10 (d, 1H, CH_2^c), 6.67-8.03 (m, 12H, ArH), 9.10 (d, 1H, H^bC=N), 9.20 (d, 1H, H^aC=N), 14.20 (s, 1H, OH^b), 14.46 (s, 1H, OH^a). UV-Vis. (acetonitrile): λ_{max} (nm), ε ($M^{-1}cm^{-1}$) = 310 (23034), 363 (10191), 406 (13193), 426 (12655).

H_2L3: N,N'-bis(naphthalidene)-1,3-propylenediamine. Yield: 77%, color: yellow, m.p. = 209-211 °C, anal. found (calc.): $C_{25}H_{22}N_2O_2$ (382.46): C, 78.76 (78.51); H, 5.74 (5.80); N, 7.75 (7.32). IR (KBr, cm^{-1}): 3446 (ν_{O-H}), 2941-3039 (ν_{C-H}), 1622 ($\nu_{C=N}$), 1541 ($\nu_{C=C}$), ^{1}H NMR (250 MHz, DMSO-d_6, room temperature): δ (ppm) = 2.06-2.21 (m, 2H, CH_2^b), 3.74-3.76 (t, 4H, CH_2^a), 6.71-8.07 (m, 12H, ArH), 9.14 (s, 2H, HC=N), 14.17 (s, 2H, OH). UV-Vis (acetonitrile): λ_{max} (nm), ε ($M^{-1}cm^{-1}$) = 262 (sh), 270 (sh), 309 (19057), 410 (13682), 424 (14659).

Synthesis of the nano uranyl Schiff base complexes

The complexes were prepared by slow addition of uranyl acetate (0.40 mmol, 0.17 g), which was dissolved in about 50 mL of methanol, into a hot 50 mL methanolic solution of stirred H_2L (0.38 mmol, 0.15 g). The addition of uranyl acetate was prolonged for about 24 h. The mixture was then refluxed for another 24 h. The precipitated solids were slowly cooled, filtered and washed with methanol and ether. TEM image showed nano-particles with sizes between 19-32 nm (Figure 2).

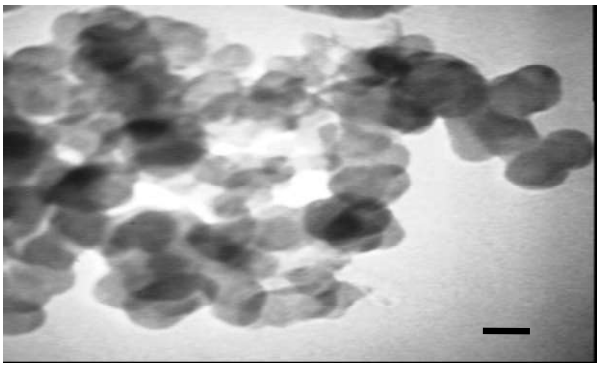

Figure 2. TEM image of nano-particles of [UO_2(L2)(MeOH)].

[UO_2(L1)(MeOH)]. Yield: 60%, color: orange, m.p. >250 °C, anal. found (calc.): $C_{25}H_{22}N_2O_5U$ (668.49): C, 45.34 (44.92); H, 3.10 (3.32); N, 4.18 (4.19). IR (KBr, cm^{-1}): 3358 (ν_{O-H}) (MeOH), 2734-3051 (ν_{C-H}), 1619 ($\nu_{C=N}$), 1540 ($\nu_{C=C}$), 885 ($\nu_{U=O}$), 644 (ν_{U-N}). ^{1}H NMR (250 MHz, DMSO-d_6, room temperature): δ (ppm) = 3.14 (d, 3H, MeOH), 4.07 (q, 1H, MeOH), 4.74 (s, 4H, CH_2), 7.24-8.37 (m, 12H, ArH), 10.33 (s, 2H, HC=N). UV-Vis (acetonitrile): λ_{max} (nm), ε ($M^{-1}cm^{-1}$) = 243 (69032), 355 (sh), 394 (sh), 315 (17609).

[UO_2(L2)(MeOH)]. Yield: 70%, color: red, m.p. >250 °C, anal. found (calc.): $C_{26}H_{24}N_2O_5U$ (682.52): C, 46.19 (45.76); H, 3.53 (3.54); N, 4.51 (4.10). IR (KBr, cm^{-1}): 3417 (ν_{O-H}) (MeOH), 2916-3070 (ν_{C-H}), 1612 ($\nu_{C=N}$), 1550 ($\nu_{C=C}$), 902 ($\nu_{U=O}$), 547(ν_{U-N}). ^{1}H NMR (250 MHz, DMSO-d_6, room temperature): δ (ppm) = 1.42-1.45 (d, 3H, CH_3^e), 3.14 (d, 3H, MeOH), 4.08 (q, 1H, MeOH), 4.67- 4.74 (d, 2H, CH_2^c), 5.15 (m, 1H, CH^d), 7.24-8.37 (m, 12H, ArH), 10.18 (s, 1H, H^bC=N), 10.33 (s, 1H, H^aC=N). UV-Vis (acetonitrile): λ_{max} (nm), ε ($M^{-1}cm^{-1}$) = 316 (sh), 365 (8732).

[UO_2(L3)(MeOH)]. Yield: 49%, color: red, m.p. >250 °C, anal. found (calc.): $C_{26}H_{24}N_2O_5U$. $0.7H_2O$ (695.12): C, 44.52 (44.93); H, 3.18 (3.68); N, 4.17 (4.03). IR (KBr, cm^{-1}): 3417 (ν_{O-H}) (MeOH), 2931-3039 (ν_{C-H}), 1612 ($\nu_{C=N}$), 1542 ($\nu_{C=C}$), 902 ($\nu_{U=O}$), 555 (ν_{U-N}). ^{1}H NMR (250 MHz, DMSO-d_6, room temperature): δ (ppm) = 2.65 (s, 2H, CH_2^b), 3.14 (d, 3H, MeOH), 4.09 (q, 1H, MeOH), 4.42-4.47 (m, 4H, CH_2^a), 7.22-8.24 (m, 12H, ArH), 10.09 (s, 2H, HC=N). UV-Vis (acetonitrile): λ_{max} (nm), ε ($M^{-1}cm^{-1}$) = 316 (sh), 365 (sh).

[UO_2(L4)(MeOH)]. It was synthesized by template method. Yield: 60%, color: orange, m.p. >250 °C, anal. found (calc.): ($C_{27}H_{26}N_2O_5U$). $2NO_3$. $1H_2O$ (838.57): C, 38.46 (38.67); H, 3.42 (3.37); N, 6.26 (6.68). IR (KBr, cm^{-1}): 3456 (ν_{O-H}), 2939-3047 (ν_{C-H}), 1628 ($\nu_{C=N}$), 1543 ($\nu_{C=C}$), 902 ($\nu_{U=O}$), 470 (ν_{U-N}). ^{1}H NMR (250 MHz, DMSO-d_6, room temperature): δ (ppm) = 4.08 (m, 4H, CH_2^b), 4.37 (m, 4H, CH_2^a), 7.13-8.19 (m, 12H, ArH), 10.13 (s, 2H, HC=N). UV-Vis (acetonitrile): λ_{max} (nm), ε ($M^{-1}cm^{-1}$) = 243 (24181), 330 (14974), 441 (sh).

X-ray structural determination of [UO_2(L3)DMF]

Crystals of [UO_2(L3)DMF] were obtained in good yield by slow evaporation of a DMF solution of [UO_2(L3)MeOH] at room temperature. The red crystal was mounted on a glass fiber and used for data collection. The data collection and reduction were performed by X-AREA program [14]. The multi-scan absorption correction was performed by MULABS routine [15]. The structure was solved by direct methods using SHELXS97 [16] and subsequent difference Fourier map and then refined by a full-matrix least-squares on F^2 by SHELXL97 in SHELXTL package [16]. The non-hydrogen atoms were refined anisotropically. All of the H atoms were positioned geometrically and constrained to ride on their parent atoms with $U_{iso}(H) = 1.2$ or $1.5U_{eq}(C)$. All refinements were performed using the SHELXTL crystallographic software package. All calculations were done using PLATON [17].

Cell culture and MTT assay for analysis of anticancer properties of the complexes

The cancer cells were cultured in RPMI 1640 Medium (HiMedia, Mumbai, India) supplemented with 10% Fetal Calf Serum (FCS) (Biochrom, Germany). Also 100 IU/mL of penicillin and 100 mg/mL of streptomycin were added to the medium as antibiotics to control the growth of contaminating microorganisms. The cells were cultured in 96-well cell culture plates (Greiner, USA), and kept at 37 °C in a humidified atmosphere of 5 percentage CO_2, in a CO_2 incubator. All the experiments were performed using Jurkat cancer cell line of 10-15 passage. The growth inhibitory effect of uranyl complexes (**L1-L4**) toward the cancer cells was measured using 3-(4,5-dimethylthiazol-2-yl)-2,5-diphenyltetrazoliumbromide (MTT) assay. Briefly, the cleavage and conversion of the soluble yellowish MTT to the insoluble purple formazan by active mitochondrial dehydrogenase of living cells has been used to develop an assay system alternative to other assays for measurement of cell proliferation [18]. The drug treatment was performed as the harvested cells were seeded into the 96-well plate (2.5×10^4 cells/well) with varying concentrations of the sterilized uranyl complexes (0-100 μM) and incubated for 24 and 48 h. Four hours to the end of incubations, 25 μL of MTT solution (5 mg/mL in PBS) was added to each well containing fresh and cultured media. At the end, the insoluble formazan produced was dissolved in solution containing 10% SDS and 50% DMF (left for 1 h at 37 °C in dark conditions) and optical density (OD) was read against reagent blank with multi well scanning spectrophotometer (ELISA reader, Bio-Tek's ELx808, USA) at a wavelength of 570 nm. The absorbance is a function of concentration of the converted dye. The OD value of study groups was divided by the OD value of untreated control and presented as percentage of control (as 100%). Also the values of IC_{50} (the concentrations required for 50% growth inhibition), after 24 h of incubation with the complexes were calculated. Cisplatin was used as a positive control on this study just to see that cytotoxic assay system is working well. The IC_{50} value of cisplatin

against this cancer cell line was about 74 μM. By considering this value, the synthetic complexes demonstrated higher anticancer activity than this standard drug.

RESULTS AND DISCUSSION

General information

A number of solvent adducts of the uranyl complexes of the Schiff base ligands such as *salen* (N,N′-ethylenebis(salicylideneimine)) and *salpn* (N,N′-propylenebis(salicylideneimine)) have been synthesized and characterized by X-ray crystallography. Evans *et al.* [9] revealed that special solvents used in the synthesis or recrystallization could coordinate to the uranium center.

Crystal structure of [UO_2(L3)(DMF)]

The solid state structure of the complex was determined by single-crystal X-ray diffraction. The ORTEP view of the complex was shown in Figure 3a. Crystallographic data and refinement parameters of the complex were listed in Table 1.

Table 1. Crystal data and structure refinement for [UO_2(L3)(DMF)]

Identification code	BE29
Empirical formula	$C_{28}H_{27}N_3O_5U$, C_3H_7NO
Formula weight	796.65
Temperature	291(2) K
Wavelength	0.71073 Å
Crystal system	Monoclinic
Space group	*P 2(1)/c*
Unit cell dimensions	a = 8.7992(18) Å α = 90°. b = 20.127(4) Å β =102.49(3)°. c = 18.168(4) Å γ = 90°.
Volume	3141.5(11) $Å^3$
Z	4
Density (calculated)	1.684 Mg/m^3
Absorption coefficient	5.214 mm^{-1}
F(000)	1552
Crystal size	0.15 x 0.11 x 0.08 mm^3
Theta range for data collection	2.02 to 29.26°.
Index ranges	-10<=h<=12, -27<=k<=27, -24<=l<=24
Reflections collected	21291
Independent reflections	8281 [R(int) = 0.0782]
Completeness to theta = 29.26°	96.7 %
Absorption correction	Semi-empirical from equivalents
Max. and min. transmission	1.000 and 0.756
Refinement method	Full-matrix least-squares on F^2
Data / restraints / parameters	8281 / 150 / 421
Goodness-of-fit on F^2	0.961
Final R indices [I>2sigma(I)]	R1 = 0.0495, wR2 = 0.0865
R indices (all data)	R1 = 0.0926, wR2 = 0.0968
Largest diff. peak and hole	2.098 and -1.677 e. $Å^{-3}$

It was found that the complex has a pentagonal-bipyramidal geometry with an axial O=U=O moiety. The coordination geometry around UO_2^{2+} was nearly planar with the dihedral angle of 5.62(2)° between coordination planes of N1-U1-O1 and N2-U1-O2. Atoms C12, C14 were

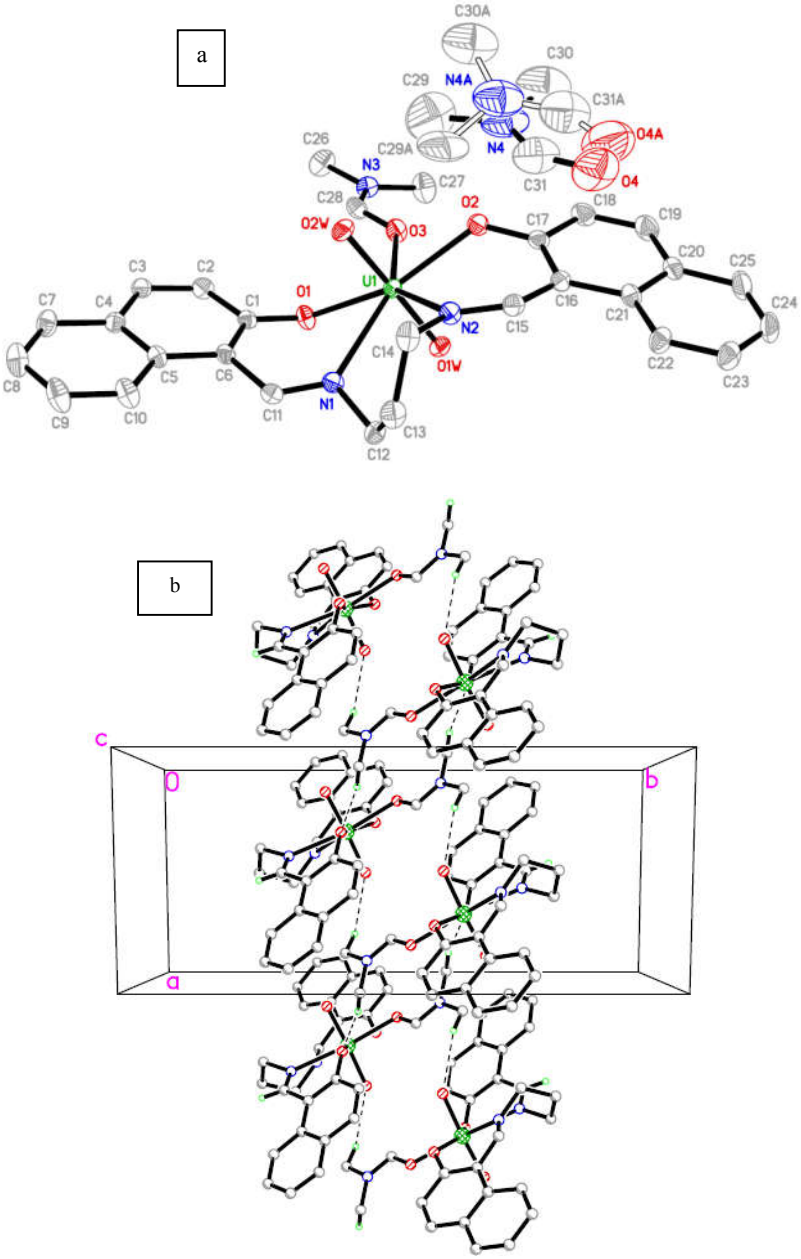

Figure 3. X-ray crystal structure (a) and crystal packing of [UO_2(L3)(DMF)] (b). Intermolecular interactions were shown as dashed lines.

significantly out of the O1-U1-O2-N1-N2 plane with maximum deviation from the mean plane of -0.86(1) and 0.79(1) Å for C12 and C14 atoms, respectively. The U=O bond distances in the

uranyl moiety were 1.787(4) Å [U(1)-O1w] and 1.790(4) Å [U(1)-O2w], which were typical values for uranyl compounds. The O(1w)-U(1)-O(2w) bond angle [176.7(2)°] indicated that the uranyl moiety was slightly bent in the direction opposite to the coordination of DMF. The bond distance between the oxygen atom of DMF and uranium was 2.449(5) Å [U(1)-O(3)] which was longer than those of U(1)-O(1) and U(1)-O(2). The dimethylformamide solvent of recrystallization was totally disordered over two positions with a refined occupancy ratio of 0.780(14)/0.220(14). The slightly low GOOF parameter is a reflection of low quality of crystal and distorted solvent molecule, while the slightly large difference peak and hole parameters is due to the presence of heavy uranium atom in the structure. The crystal packing of the complex showed one dimensional infinite chain through C–H···O interactions along the *c*-axis (Figure 3b).

Infrared spectra

The IR spectra of the ligands and their complexes were found to be quite complex because of large number of bands of varying intensities. In the IR spectra of the ligands ν_{OH} broad band appeared in the 3358-3469 cm^{-1} range [19]. After formation of the uranyl complexes, these bands were disappeared but they were still seen because of the coordinated methanol. The bands at 2734-3070 cm^{-1} in the Schiff base ligands and complexes were assigned to aliphatic and aromatic C-H modes of vibrations. The peak of azomethine group at 1612-1637 cm^{-1} of the free Schiff base ligand was shifted to lower frequencies in the spectra of the uranyl complexes [20]. Coordination of the Schiff base ligands to the uranyl center through the nitrogen atom was expected to reduce the electron density in the azomethine link and lowers the stretching vibrational motion of $\nu_{C=N}$. Stretching vibrations of C=C of the benzene ring were appeared in the range 1540-1550 cm^{-1} [21]. The stretching vibration of $\nu_{U=O}$ was observed in the range 855-902 cm^{-1}. The bands at 540-644 cm^{-1} in the complexes were assigned to (ν_{U-N}) vibrations.

^{1}H NMR spectra

In the ^{1}H NMR spectra of the ligands, signals in the range 14.17-14.46 ppm were assigned to the hydroxyl protons of 2-hydroxy-1-naphthaldehyde. In the ^{1}H NMR spectra of the complexes the absence of these signals showed that the ligands were coordinated to the metal. The azomethine groups were appeared in the range 9.10-10.34 ppm. For the symmetrical Schiff bases, it was supposed to see only one chemical environment (as a singlet), but for the asymmetrical Schiff bases two signals were seen. Aromatic rings protons were shown in the range 6.67 to 8.43 ppm and they were weakly affected by complexation. Aliphatic protons were appeared within the range 1.34-5.15 ppm. Moreover, it was reported that the special solvent molecule in the fifth position of the equatorial plane was completely depend on the solvent which was used for the synthesis or recrystallization. It was confirmed that by changing the solvent of the synthesis or recrystallization, the coordinated solvent was changed [9]. All ^{1}H NMR of the complexes were monitored in DMSO-d_6 solvent, thus it was reasonable that DMSO-d_6 repelled methanol from the coordination sphere, thus coordinated to the vacant site. Peaks due to free MeOH were observed in the ^{1}HNMR as a quartet at about 4.12 ppm related to OH and a doublet at about 3.15 ppm related to CH_3 [22].

Electronic spectra

For the free ligand, the band in the region 300-500 nm was attributed to the n→π* transition due to involving molecular orbitals of the -CH=N chromophore, and the bands in the higher energy region at 200-300 nm were assigned to the π→π* transition. The first bands at higher energy were attributed to π→π* transitions associated with the phenyl ring and the second bands at lower energy were arised from n→π* transitions associated with the azomethine chromophore.

Since uranyl complexes contain U(VI) with an empty valence shell the metal center was only capable to function as acceptor site for LMCT transitions. There were two kinds of charge transfer bands in the uranyl complexes; electron transfer from the axial oxygens to the central metal (2p of oxygen to 5f), and electron transfer from the phenolate group of the Schiff base ligand to the metal. It was believed that charge transfer band from axial oxygens to the central metal was occurred at lower frequencies than the Schiff base oxygen to U(VI). The bands in the region 300-600 nm were assigned to the LMCT transition.

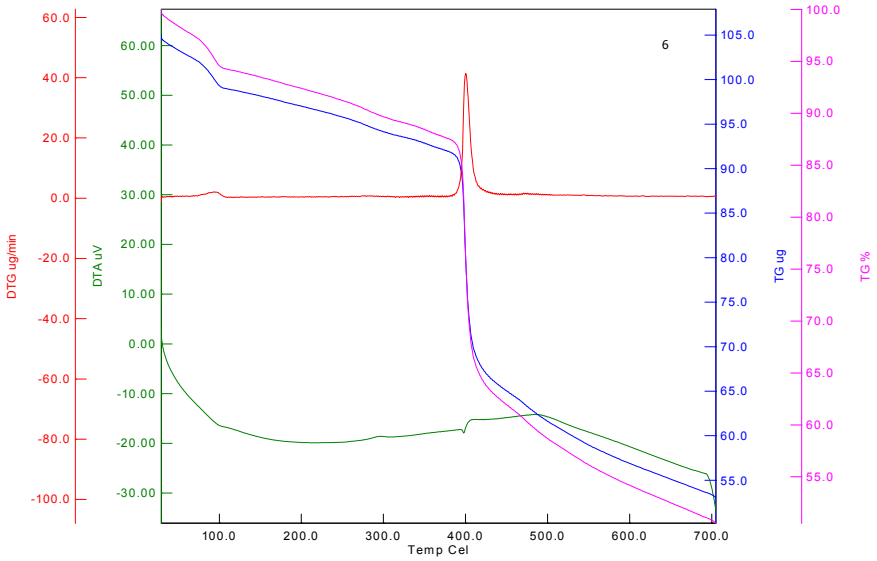

Figure 4. TG, DTA and DTG of $[UO_2(L3)(MeOH)]$.

Table 2. Thermal analysis data of the uranyl complexes.

Complex (F.W.)	TGA (Wt. loss %) calc. (found)	Temp range in TG (°C)	Decomposition assignment
$[UO_2(L1)(MeOH)]$ $C_{25}H_{22}N_2O_5U$ (668.49)	4.8 (5.0) 4.2 (3.5)	185-240 395-450	Loss of MeOH Loss of C_2H_4
$[UO_2(L2)(MeOH)]$ $C_{26}H_{24}N_2O_5U$ (682.52)	4.7 (5.5) 36.9 (35.5)	220-270 380-455	Loss of MeOH Loss of $C_{20}H_{12}$
$[UO_2(L3)(MeOH)]$ $C_{26}H_{24}N_2O_5U$ (682.00)	4.7 (5.5) 6.2 (8.0)	< 104 385-419	Loss of MeOH Loss of C_3H_6
$[UO_2(L4)(MeOH)]$ $C_{27}H_{26}N_2O_5U$ (696.00)	20.4 (21.0)	250-360	Loss of MeOH and $C_6N_2H_{10}$

Thermal studies

Thermal properties of the metal complexes were investigated up to 1000 °C range under nitrogen atmosphere at a heating rate of 10 °C/min. As an example, the TG, DTA and DTG curves of $[UO_2(L3)(MeOH)]$ are shown in Figure 4. The thermogram of this complex showed that it decomposed in two steps. In the first step, it lost 5.5% of its weight with the separation of a molecule of methanol at 104 °C and in the second step the removal of the C_3H_6 occurred at 385-419 °C with 8.0% weight loss. Also in other complexes the first step was attributed to the

release of the coordinated methanol and occured below 270 °C. Uranyl complexes had different thermal stabilities. The temperature ranges and the percentages of the weight loss were given in Table 2.

Kinetic aspects of thermal decomposition

DTG curves were used to study the kinetics of decomposition of the complexes and inorder to calculate kinetic parameters, Coats-Redfern equation (1) was used [23].

$$\log\left[\frac{-\log(1-a)}{T^2}\right] = \log\frac{A*R}{\beta E}\left[1-\frac{2RT}{E}\right] - \frac{E}{2.303RT} \quad (1)$$

In this equation; $a = \frac{(w_0-w_t)}{(w_0-w_f)}$. w_0 = initial mass of the sample; w_t = mass of the sample at temperature T; w_f = the final mass at a temperature when the mass loss was approximately unchanged; β = the heating rate; R = the gas constant. A plot of log $[\frac{-\log(1-a)}{T^2}]$ against 1/T gave a straight line with the slope of –E/2.303R. A* values could be calculated from the intercept of this plot and the entropy of activation ($\Delta S^{\#}$) were obtained using equation (2):

$$A* = \frac{KT_s}{h} e^{S^{\#}/T} \quad (2)$$

where h = the Planck constant, K = the Boltzmann constant and T_s= the peak temperatureobtained from DTG. The enthalpy and free energy of activation were calculated using equations (3 and 4):

$$E = H^{\#} + RT \quad (3)$$

$$G^{\#} = H^{\#} - TS^{\#} \quad (4)$$

Activation parameters obtained for all the complexes were presented in Table 3. From these data it could be concluded that the Gibbs energy grew from stage to stage. This was probably due to the stable intermediate of the present stages. According to Coats-Redfern plots, in these complexes the kinetic of thermal decomposition was first-order in all stages.

Table 3. Thermal and kinetic parameters of decomposition of the uranyl complexes.

Complex	$\Delta T(^oC)^a$	E* ($kJmol^{-1}$)	A* (s^{-1})	S* ($Jmol^{-1}K^{-1}$)	H* ($kJmol^{-1}$)	G* ($kJmol^{-1}$)
$[UO_2(L1)(MeOH)]$	185-240	50.87	5.02×10^5	-139.85	46.83	29.94
	395-450	40.79	7.63×10^3	-177.43	35.13	72.27
$[UO_2(L2)(MeOH)]$	220-270	70.82	1.34×10^7	-113.20	66.42	28.97
	380-455	41.23	6.75×10^3	-178.62	35.45	75.35

[a]The temperature range of decomposition pathways.

Electrochemical studies of the uranyl complexes

Electrochemical cyclic voltammetry measurements of the uranyl complexes (1.0 mM) in acetonitrile with 0.1 M TBAP were made over a potential range between 0.2 V to −1.4 V. TBAP was used as a supporting electrolyte. A reduction peak was observed ca. −0.93 V and it showed a quasi reversible one-electron step. Upon reversal of the scan direction, the U(V) complex was oxidized to U(VI) at more anodic potentials. The U=O bond strength in the uranyl moiety was weakened with the reduction. The formal potentials ($E_{1/2}$(VI↔V)) for the U(VI/V) redox couple were calculated as the average of the cathodic (E_{pc}) and anodic (E_{pa}) peak potentials of this

process. By considering data in Table 4, it was obvious that a one electron quasi reversible oxidation was occurred [24, 25].

Table 4. Redox potential data of uranyl complexes in acetonitrile solution.

Complex	Ep_a(V→ VI)	Ep_c(VI→ V)	$E_{1/2}$(V↔VI)
$[UO_2(L1)(CH_3CN)]$	-0.784	-0.930	-0.857
$[UO_2(L2)(CH_3CN)]$	-0.695	-0.865	-0.780
$[UO_2(L3)(CH_3CN)]$	-0.763	-0.997	-0.880
$[UO_2(L4)(CH_3CN)]$	-0.796	-0.957	-0.876

Structure-activity relationship of the uranyl complexes

Anticancer activities of the complexes were investigated. It was found that although these compounds with aliphatic bridging units exhibited significant cytotoxic activities, the complexes with aromatic bridging units, as it was studied before by our group, demonstrated more significant anticancer activities [13]. The obtained results could be explained with the different dynamics of molecular structures, as more rigid structures were in favor of displaying better anticancer properties. Among the complexes with aliphatic bridging units, 1,4-butylenediamine bearing complexes displayed the least anticancer activities, which could be explained with higher flexibility and dynamic structures (Table 5 and Figure 5).

Table 5. The IC_{50} values (μM) of the complexes against Jurkat cell line.

Complex	**1**	**2**	**3**	**4**
IC_{50}	49	6.12	10.15	--

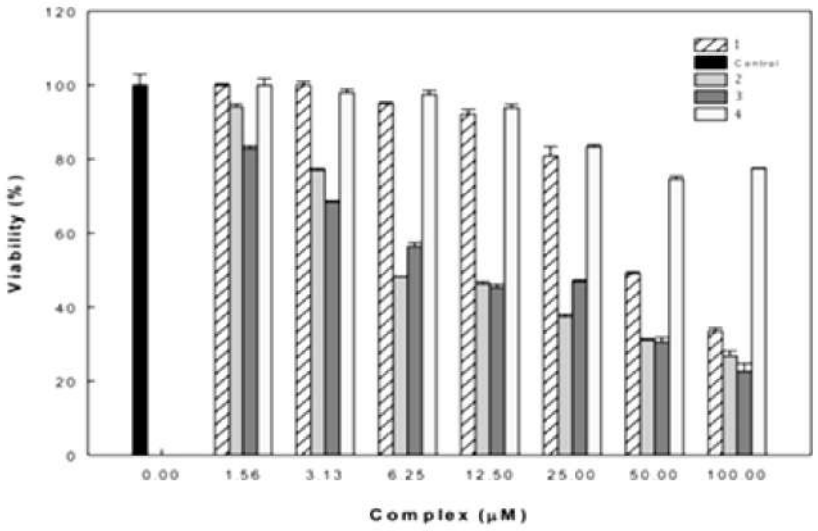

Figure 5. Growth inhibition of the compounds investigated on Jurkat cell line for 24 h. Cell viability was evaluated by the MTT colorimetric assay. The vertical bars represented standard deviation (SD) of the triplicate determinations. 1: $[UO_2(L3)(MeOH)]$, 2: $[UO_2(L2)(MeOH)]$, 3: $[UO_2(L1)(MeOH)]$, 4: $[UO_2(L4)(MeOH)]$.

CONCLUSIONS

This study involved the synthesis of a range of nano uranyl Schiff base complexes. By evaluating the X-ray structure of $[UO_2(L3)(DMF)]$, it was found that one solvent molecule (DMF) was coordinated weakly to the uranium center. Two other DMF molecules did not show any coordination to $[UO_2(L3)(DMF)]$, but they were just present as solvent in the crystal structure. Furthermore, the presence of one coordinated solvent molecule was confirmed by thermal gravimetric studies. Cyclic voltammetry was used to investigate the reduction and oxidation of uranium $U^{(VI)} \leftrightarrow U^{(V)}$. Kinetics of thermal decomposition was investigated to study the behavior of these complexes in the solid-state. Kinetic's parameters (the activation energy E* and the pre-exponential factor A*) were reported and the negative values of the entropy of activation confirmed that the activated complex had a more ordered structure than the reactants. According to Coats-Redfern plots the kinetics of thermal decomposition of the studied complexes was first-order in all stages. All the complexes except **L4** had high anticancer efficiency.

ACKNOWLEDGEMENT

We are grateful to Shiraz University Research Council for its financial support.

Supplementary material

CCDC number 860315 contains the supplementary crystallographic data for this paper. These data can be obtained free of charge from The Cambridge Crystallographic Data Centre via www.ccdc.cam.ac.uk/data_request/cif.

REFERENCES

1. Cozzi, P.G. Metal–Salen Schiff base complexes in catalysis: Practical aspects. *Chem. Soc. Rev.* **2004**, 33, 410-421.
2. Abdel-Aziz, A.A. Synthesis, spectroscopic characterization, thermal studies, catalytic epoxidation and biological activity of chromium and molybdenum hexacarbonyl bound to a novel N_2O_2 Schiff base. *J. Mol. Struct.* **2010**, 979, 77-85.
3. Atwood, D.A. Salan complexes of the group 12, 13 and 14 elements. *Coord. Chem. Rev.* **1997**, 165, 267-296.
4. Gibson, V.C.; O'Reilly, R.K.; White, A.J.P.; Williams, D.J. Design of highly active iron-based catalysts for atom transfer radical polymerization: Tridentate salicylaldiminato ligands affording near ideal Nernstian behavior. *J. Am. Chem. Soc.* **2003**, 125, 8450-8451.
5. Bu, J.; Judeh, Z.M.A.; Ching, C.B.; Kawi, S. Epoxidation of olefins catalyzed by Mn(II) salen complex anchored on PAMAM–SiO_2 dendrimer. *Catal. Lett.* **2003**, 85, 183-187.
6. Shebl, M. Synthesis and spectroscopic studies of binuclear metal complexes of a tetradentate N_2O_2 Schiff base ligand derived from 4,6-diacetylresorcinol and benzylamine. *Spectrochim. Acta Part A* **2008**, 70, 850-859.
7. Asadi, M.; Barzegar Sadi, S.; Asadi, Z.; Yousefi, R.; Barzegar Sadi, A.R.; Khalili Hezarjaribi, H. Synthesis, characterization and the interaction of some new water-soluble metal Schiff base complexes with human serum albumin. *J. Coord. Chem.* **2012**, 65, 722-739.
8. Mohamed, G.G.; Omar, M. M.; Hindy, A.M.M. Synthesis, characterization and biological activity of some transition metals with Schiff base derived from 2-thiophene carboxaldehyde and aminobenzoic acid. *Spectrochim. Acta Part A* **2005**, 62, 1140-1150.
9. Evans, D.J.; Junk, P.C.; Smith, M.K. The effect of coordinated solvent ligands on the solid-state structures of compounds involving uranyl nitrate and Schiff bases. *Polyhedron* **2002**, 21, 2421-2431.

10. Takao, K.; Tsushima. S.; Takao, S.; Scheinost, A.C.; Bernhard, G.; Ikeda, Y.; Hening, C. X-ray absorption fine structures of uranyl(V) complexes in a nonaqueous solution. *Inorg. Chem.* **2009**, 48, 9602-9604.
11. Gaunt, A.J.; May, I.; Copping, R.; Bhatt, A.I.; Collison, D.; Fox, O.D.; Holman, K.T.; Pope, M.T. A new structural family of heteropolytungstate lacunary complexes with the uranyl, UO_2^{2+}, cation. *Dalton Trans.* **2003**, 15, 3009-3014.
12. Bharara, M.S.; Strawbridge, K.; Vilsek, J.Z.; Bray, T.H.; Gorden, A.E.V. Novel dinuclear uranyl complexes with asymmetric Schiff base ligands: Synthesis, structural characterization, reactivity, and extraction studies. *Inorg. Chem.* **2007**, 46, 8309-8315.
13. Asadi, Z.; Asadi, M.; Dehghani-Firuzabadi, F.; Yousefi, R.; Jamshidi, M. Synthesis, characterization, anticancer activity, thermal and electrochemical studies of some novel uranyl Schiff base complexes. *J. Iran. Chem*. Soc. **2014**, 11, 423-429.
14. Stoe&Cie, X–AREA, V 1.30, *Program for the Acquisition and Analysis of Data; Stoe & Cie GmbH:* Darmstadt, Germany; **2005**.
15. Blessing, R.H. An empirical correction for absorption anisotropy. *Acta Cryst. A* **1995**, 51, 33-38.
16. Sheldrick, G.M. A short history of *SHELX*. *Acta Cryst. A* **2008**, 64, 112-122.
17. Spek, A.L. Structure validation in chemical crystallography. *Acta Cryst. D* **2009**, 65, 148-155.
18. Mossman, T. Rapid colorimetric assay for cellular growth and survival: Application to proliferation and cytotoxicity assays. *J. Immunol. Methods* **1983**, 65, 55-63.
19. Dehghani-Firuzabadi, F.; Asadi, Z.; Panahi, F. Immobilized NNN Pd-complex on magnetic nanoparticles: Efficient and reusable catalyst for Heck and Sonogashira coupling reactions. *RSC Adv.* **2016**, **6**, 101061-101070.
20. Paulpandiyan, R.; Raman, N. DNA binding propensity and nuclease efficacy of biosensitive Schiff base complexes containing pyrazolone moiety: Synthesis and characterization. *J. Mol. Struct*. **2016**, 1125, 374-382.
21. Mandegani, Z.; Asadi, Z.; Asadi, M.; Karbalaei-Heidari, H.R.; Rastegari, B. Synthesis, characterization, DNA binding, cleavage activity, cytotoxicity and molecular docking of new nano water-soluble $[M(5\text{-}CH_2PPh_3\text{-}3,4\text{-salpyr})](ClO_4)_2$ (M = Ni, Zn) complexes. *Dalton Trans.* **2016**, 45, 6592-6611.
22. Asadi, Z.; Golzard, F.; Eigner, V.; Dusek, M. Synthesis, X-ray crystallography, spectroscopy, electrochemistry, thermal and kinetic study of uranyl Schiff base complexes. *J. Coord. Chem*. **2013**, 66, 3629-3646.
23. Coats, A.W.; Redfern, J.P. Kinetic parameters from thermogravimetric data. *Nature* **1964**, 201, 68-69.
24. Morris, D.E. Redox energetics and kinetics of uranyl coordination complexes in aqueous solution. *Inorg. Chem*. **2002**, 41, 3542-3547.
25. Asadi, Z.; Asadi, M.; Dehghani-Firuzabadi, F.; Ranjkesh-Shorkaei, M. New method in synthesis of nano uranyl(VI) Schiff base complexes: Characterization and electrochemical studies. *J. Ind. Eng. Chem*. **2014**, 20, 4227-4232.